The orientation dependence of the hydrogen distribution within Mo/V (110) and (001) multilayered artificial superlattices

1997 J. Phys.: Condens. Matter 9 73

(http://iopscience.iop.org/0953-8984/9/1/010)

J. Phys.: Condens. Matter **9** (1997) 73–85. Printed in the UK PII: S0953-8984(97)73626-9

The orientation dependence of the hydrogen distribution within Mo/V (110) and (001) multilayered artificial superlattices

B Hjörvarsson†, J Birch‡, F Stillesjö†, S Ólafsson†, J-E Sundgren‡ and E B Karlsson†

† Department of Physics, Uppsala University, Box 530, S-751 21 Uppsala, Sweden
‡ Department of Physics, Linköping University, S-581 83 Linköping, Sweden

Received 15 April 1996, in final form 16 September 1996

Abstract. We have investigated the hydrogen distribution within multilayered Mo/V (110) and (001) artificial superlattices. The hydrogen concentration, determined by the $^{1}H(^{15}N, \alpha\gamma)^{12}C$ nuclear resonance reaction, is found to decrease with decreasing layer thickness. The decrease is attributed to an interface region with reduced hydrogen content. The extension of this interface region is found to be two monolayers in Mo/V (110), compared to the previously reported three monolayers in Mo/V (001) superlattices. In the (110) oriented samples the relative amount of H in the interface region decreases with increasing average H content (H/V (atomic ratio) $\approx$ 0.3–0.5). This effect is shown to be related to the orientation of the hydrogen planes with respect to the boundaries implied by the Mo/V interfaces. The hydrogen induced volume change, obtained by conventional θ–2θ x-ray diffraction (XRD) and reciprocal space mapping, is found to be smaller for the (110) samples than for the (001) oriented samples at room temperature.

1. Introduction

The interest in hydrogen in multilayers and superlattices is partially motivated by the possibility of investigations of physical phenomena in reduced dimensionality. The pioneering investigations of interaction of hydrogen with artificial superlattices were performed by Micheli, Zabel and co-workers [1–4]. Their investigations of the Nb–Ta superlattices revealed many novel phenomena related to the finite size of the host material, including hydrogen induced strain modulation [1], hydrogen phase related critical fluctuations [2, 3], and resistivity changes upon hydrogen loading [4]. The hydrogen uptake and the associated lattice changes for Mo/V (001) samples have been previously investigated by the present authors [5–8]. The main difference between the Mo/V and the Nb–Ta superlattices is the modulation of the hydrogen concentration. The absorption potentials in Nb and Ta are similar and give rise to only a weak modulation in the hydrogen concentration, at all but low temperatures. For Mo/V, the difference in the absorption potential is exceptionally large, which implies that the hydrogen is exclusively located in V in a broad temperature range [5–8].

One of the key parameters of the heat of solution for H in metals is the interstitial electron density. When Mo/V superlattices are grown epitaxially, the coherency strain causes the

0953-8984/97/010073+13$19.50

lattice parameter perpendicular to the growth direction to increase in V and decrease in Mo, compared to their bulk values. If not compensated by contraction and expansion, respectively, in the growth direction, the interstitial electron density will be increased in Mo and decreased in V. Thus both electron transfer and non-isotropic lattice parameter changes can be expected in epitaxially grown Mo/V superlattices [8]. In an article focusing on the superconducting properties of Mo/V superlattices Ariosa, Triscone and coworkers [9] reported an abrupt change in T_c, at a superlattice wavelength (Λ) $\approx$ 32 monolayers for both the (110) and the (001) oriented samples. The ratio of the atomic plane distances is $\sqrt{2}$, i.e. the transition scaled as the number of atomic planes of V, and not as the V layer thickness. A trilayer model, including a mixing region at the interfaces was proposed [10], which was supported by successful simulation of the XRD data. The model failed, however, to reproduce the abrupt change in T_c at $\Lambda \approx 32$ monolayers. Later this feature was shown to be related to different growth modes of the samples [11]. The abrupt change in the superconducting properties occur in the thickness range where the roughening transition of V is reached [12–14].

In this paper we present the results from equilibrium studies of hydrogen absorption in multilayered Mo/V (110) and (001) superlattices, and we use the obtained results to deduce the difference in the extension of the charge transfer for the two orientations. The difference in the hydrogen uptake of these samples is addressed as well as the structural changes imposed by the hydrogen. The relation between the local distortion of the lattice and the boundary conditions is treated in a phenomenological manner, and we show that the hydrogen induced expansion of Mo/V is strongly dependent on the orientation.

2. Experimental details

The (001) and (110) oriented Mo/V superlattices were grown on polished MgO(001) and $Al_2O_3(11\bar{2}0)$ substrates ($10 \times 10 \times 0.5$ mm^3), respectively, by dual-target magnetron sputtering. A detailed description of the deposition procedure has been published elsewhere [15]. Several superlattices with different Λ, but with the same ratio of Mo/V layer thicknesses, were consecutively deposited onto MgO and Al_2O_3 substrates. Thus, each of these multilayered superlattices effectively contained several subsamples, as illustrated in figure 1. Some of the (001) and (110) superlattices were grown simultaneously to ensure identical growth conditions. The samples were exposed to hydrogen at pressures between 0.1 and 10 bar and temperatures between 225 and 400 °C. After hydrogen loading, the samples were rapidly cooled to room temperature, and thereafter exposed to air. The V oxide formed on the surface hindered outflow of hydrogen from the samples. The samples were later introduced into a scattering chamber at the tandem accelerator in Uppsala, and rapidly cooled down to 90 K. The hydrogen content of all the subsamples was determined by the ^{15}N depth profiling method [5, 7]. These analyses were made in order to determine the extension of the hydrogen depleted interface regions for the two crystallographic orientations. By this multilayered sample approach, we were able to exclude all experimental variations in the hydrogen exposure of the samples with different Λ, as the subsamples are confined in one and the same sample. The measured hydrogen distribution within the samples resembles the thermodynamic equilibrium around room temperature.

Single-Λ samples of both (110) and (001) orientations were made for XRD analyses of the hydrogen induced lattice changes. Here we focus on the results from the (110) oriented Mo/V 16–16 monolayer samples, and refer to the relevant references for detailed information on the other orientation. The procedure for the hydrogen loading was the same as described above for the multilayered samples.

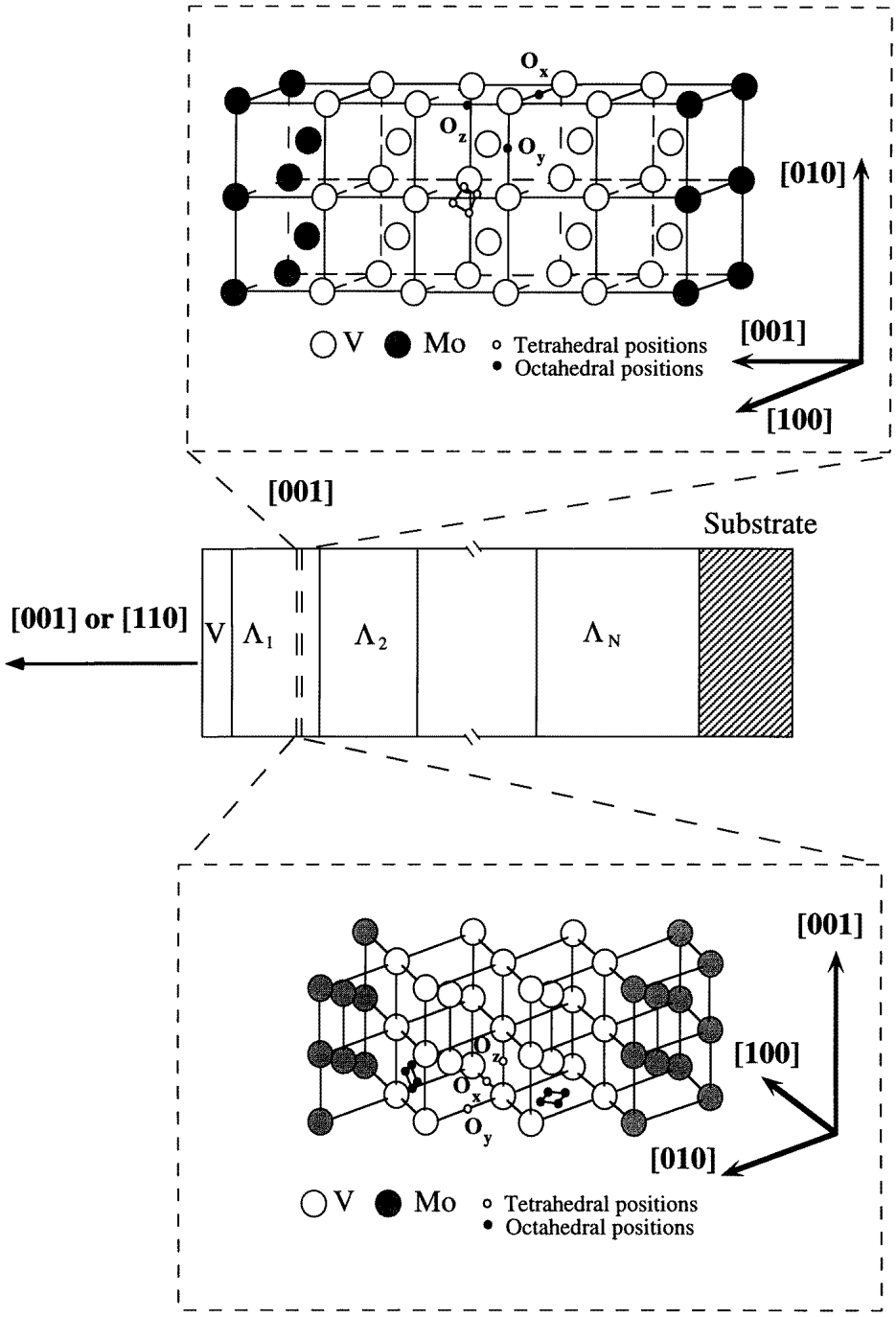

Figure 1. A schematic illustration of the multilayered superlattice (MLSL) and the crystallographic configuration for the Mo/V (001) and (110) samples. The distance between atomic planes is $\sqrt{2}$ larger for (110). The ordered bulk-like β-phase implies occupation of interstitial positions in every second (110) atomic plane.

Samples consisting of one modulation wavelength were analysed by θ–2θ XRD using a Bragg–Brentano diffractometer with a resolution of 0.01° in 2θ. Reciprocal space mapping by XRD was used to determine the average lattice parameters, parallel to the plane of the Mo and V layers as well as perpendicular to the plane in all the samples. A Philips MRD instrument, operated in the low-resolution (0.27° in 2θ) parallel beam x-ray optics mode, was used for these measurements. A more detailed description of the technique used is given elsewhere [16].

3. A model for the variation of the hydrogen concentration in superlattices containing several subsamples

The hydrogen content of a sample is conveniently expressed as an atomic ratio, i.e. the total number of hydrogen atoms divided by the number of other atoms. As a metallic superlattice can be treated as a one-dimensional array of atomic planes, the average hydrogen content can be obtained by a summation of the hydrogen content of the atomic planes perpendicular to the growth direction and division by the number of metal atoms. In thermodynamic equilibrium, the summation can be reduced to one modulation period, Λ, since all possible configurations are confined therein. Further simplification is obtained as the hydrogen content of the Mo layers is negligible. The next step is to divide the V layers into three regions, the interior region where the average hydrogen concentration in each plane is assumed to be the same, and the interface regions at each interface where the hydrogen content is deviating from that of the interior region. The resulting relation between the hydrogen content and Λ reads

$$\langle C\rangle_\Lambda = \frac{1}{n}\left[\sum_{j=1}^{n_{int}} C_j^H + [n_V - 2n_{int}]C_V^H + \sum_{j=n_n-n_{int}}^{n_v} C_j^H\right] \tag{1}$$

where $\langle C\rangle_\Lambda$ is the average hydrogen content within one period, j is the index of summation (atomic planes), and C_j^H the hydrogen to metal (H–M) ratio in the atomic plane j. The number of atomic planes in one modulation period is $n(n = n_V + n_{Mo})$, and n_{int} is the number of interface planes at each of the interfaces.

In the actual experiments the thicknesses of the constituents were not restricted to integer number of atomic planes. Therefore there are fluctuations of ± 1 monolayer present in each layer. To incorporate this, equation (1) above is replaced by a double summation, taking into account the thickness variation of the Mo and the V layers. As there are two interfaces in each modulation period, which we assume to be identical, we simply reduce the summation to one interface and multiply by two. By using the identity $\langle n_V\rangle d_V + \langle n_{Mo}\rangle d_{Mo} = L_{Mo} + L_V = \Lambda$ (L_x is the average thickness of layer x), and rearranging, one obtains

$$\langle C\rangle_\Lambda = C_V^H \frac{(1 - 2n_{int}d_V/L_V)}{1 + L_{Mo}/L_V} + \frac{d_V}{L_V}\frac{2}{1 + L_{Mo}/L_V}\sum_{j=1}^{n_{int}} C_j^H \tag{2a}$$

$$\langle C\rangle_\Lambda \approx A(1 - B/L_V) + D/L_V \tag{2b}$$

where A, B and D are constants. Equation (2a) is valid for any ratio of the constituents, when $L_V \geqslant 2n_{int}d_V$. The extension of the interface region is $n_{int}d_V$. When the L_{Mo}/L_V ratio is constant and the hydrogen is preferentially located in one of the atomic planes at the interfaces, equation (2b) is valid, and it becomes clear that the hydrogen concentration scales as the inverse thickness of the V layers. If $\langle C\rangle_\Lambda$ is plotted versus $1/L_V$ and the hydrogen content of the interface layers is zero ($D = 0$ in equation (2b)), the intercept at

the x axis gives directly the extension of the interface region. The y-intercept gives the H/V ratio in the interior region, independent of the hydrogen content of the interface layer.

4. Experimental results

4.1. Variation of the hydrogen concentration in superlattices containing several subsamples

In figure 2, we display representative hydrogen concentration profiles for (110) and (001) oriented Mo/V multilayered superlattices. The modulation wavelengths of the sublattices are, from surface to substrate, 9.2, 2.4, 3.7, 4.9, 6.1 and 7.4 nm. The Mo/V ratio is equal to 1.0. The modulation wavelengths of the (001) and (110) samples are identical since they are grown at the same occasion, while the ratio of the number of atomic planes is $\sqrt{2}/1$. These plots were chosen for comparison as the hydrogen concentration is similar in the coherent part of the samples. As seen in the figure, there are large differences in the hydrogen distribution within these samples. The decrease of the hydrogen content in the (001) oriented sample above 4.9 nm coincides with the roughening transition of V. This decrease reflects the less energetically favourable positions for H in the subsamples with large repeat lengths. This decrease is not observed in the (110) oriented samples as the roughening transition occurs at larger periods, but with the same number of atomic planes. The hydrogen uptake is less favourable in the (110) oriented samples at these concentrations. The exposure temperature was 350 °C, compared to 225 °C for the (110) oriented sample. When (001) samples are exposed to hydrogen under the same conditions as the (110) sample (0.1 bar, 225 °C), the H/V ratio is found to be much larger (close to one) in the interior region of the samples.

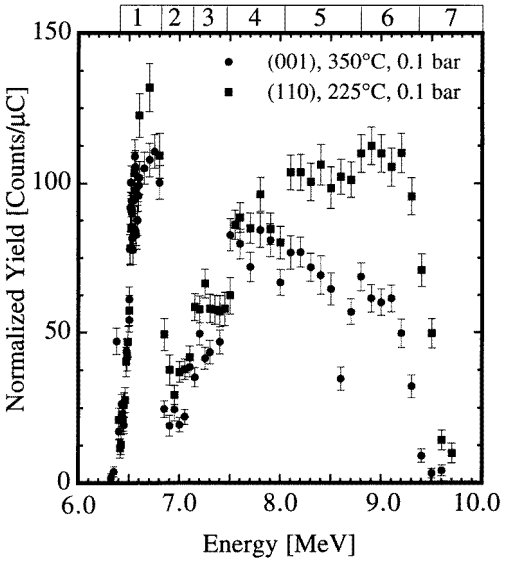

Figure 2. The hydrogen concentration profiles of multilayered (001) and (110) oriented Mo/V superlattices, with the same thicknesses of the repeat length and the sublayers. These samples were hydrogenated at the same pressure, 0.10 bar, but at different temperatures ((110) at 225 °C and (001) at 350 °C). The illustration at the top of the figure represents schematically the sample structure with (number (Λ in nm)): 1 (9.2), 2 (2.4), 3 (3.7), 4 (4.9), 5 (6.1), 6 (7.4) and finally No 7, which is the substrate.

The equilibrium concentration of hydrogen in some representative, coherently grown subsamples of (110) and (001) orientations is illustrated in figure 3. The lines in the graph are the results from fitting equation (2*a*) to the data. The fitting has a unique solution when the concentration in the interface region is restricted to be larger than zero and lower than in the interior region and all the hydrogen atoms in the interface region are assumed to be located in one atomic plane. For the (001) samples, the extension of the interface region remains at three monolayers for all concentrations up to close to stochiometric VH in the interior region. In the (110) oriented samples, the extension of the interface region is determined to be two monolayers at an H/V ratio around 0.1 (see figure 3). When the total hydrogen content increases in the (110) sample, surprisingly, the relative hydrogen content of the interface region decreases with respect to the interior region of V.

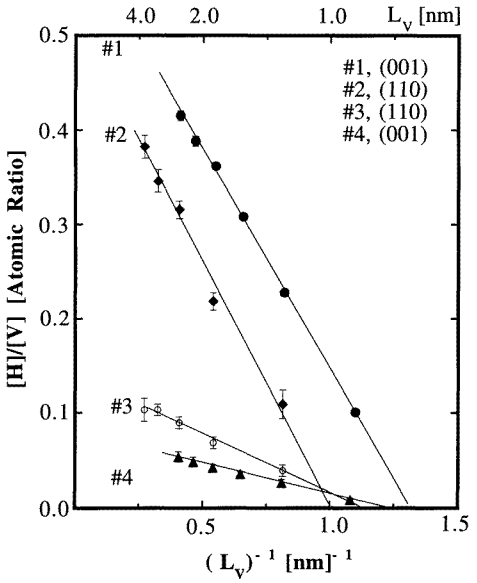

Figure 3. The hydrogen content of representative multilayered (001) and (110) oriented Mo/V samples. The concentration scales as the inverse thickness of the hydrogen containing layer. The intercept on the *y*-scale gives the hydrogen concentration in the interior layer. The lines are the results from fitting equation (2*a*) to the data. Note that the lines No 2 and No 3 cross each other. This implies that the relative hydrogen content of the interface decreases.

The (001) samples, with an average H/V ratio in the range 0.1–0.4, did not obey the simple relation (equation (2)) introduced in section 3 above. There was a strong enrichment of hydrogen in the long-modulation-wavelength region of the samples [7]. No such enrichment was observed for the (110) oriented samples at any of the measured concentrations. In figure 4, we display the relation between the concentration in the interior region of the V layers and the deduced concentration in the third monolayer from the Mo interface, for both orientations. The average concentration in the interface region is obtained by dividing by a factor of three.

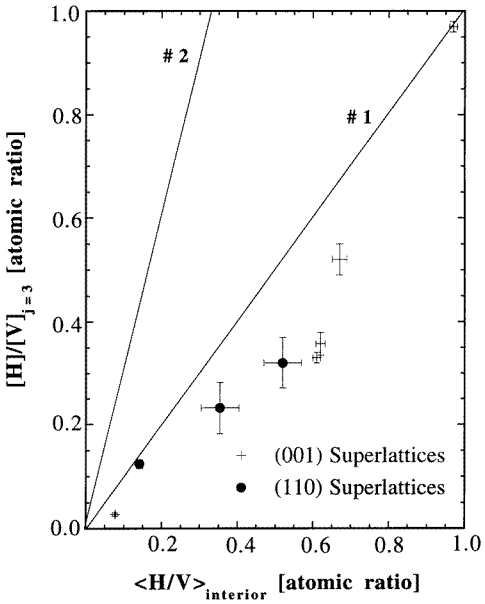

Figure 4. The deduced H/V ratio in the third atomic plane of V as a function of the average H/V ratio in the interior region of the V layers. The line marked #1 corresponds to two monolayers with H/V = 0 and the same concentration in the third layer as the interior region. The line marked #2 corresponds to equal population of the interface and the interior region.

4.2. Hydrogen induced structural changes

θ–2θ XRD and RSM were performed on all samples at room temperature. Figure 5 shows θ–2θ scans from a 16–16 monolayer Mo/V (110) sample before and after hydrogen loading (H/V = 0.50), as well as after desorption of hydrogen from the sample. As seen in the graph, the hydrogen induced structural changes are small and reversible. The strongest peak in figure 5(b) is the $11\bar{2}0$ Al_2O_3 peak; all other peaks originate from the superlattice. The Bragg peaks are labelled 110 in the figure. The Bragg peak shift towards lower angles, indicating an increase in the weighted averages of the lattice parameters in the direction perpendicular to the layers. The width of the Bragg peak increases upon hydrogen loading, from an FWHM $\approx 0.35^\circ$ to 0.65°. The separation between the superlattice satellites decreased which shows that Λ increased. The in-plane lattice parameters were unaffected by the hydrogen loading. Bulk V_2H is known to form a tetragonal lattice with the c-parameter about 9% larger, and the a-parameter 1% smaller, than the bulk lattice parameter of bcc V ($a_0 = 0.3023$ nm). The V expansion in the (110) oriented superlattice, with H/V = 0.5, was approximately 3% in the [110] direction, which is about one half of the bulklike value of $9\%/\sqrt{2} \approx 6\%$, if the tetragonal bulk V_2H unit cell with the c-axis in the [001] or the [010] direction is assumed and ignoring the change in the elastic response of the host lattice. If the volume of the hydride unit cell were conserved, the expansion would be ≈6.8%. In (001) oriented samples with equal thickness of the bilayers, the V layers are found to expand on average by 4.6% for $\langle H/V \rangle = 0.50(3)$, at room temperature [17]. The relative hydrogen induced volume change of the (110) samples compared to the (001) samples is therefore 0.65 ((3/0.50)/(4.6/0.50)) at room temperature.

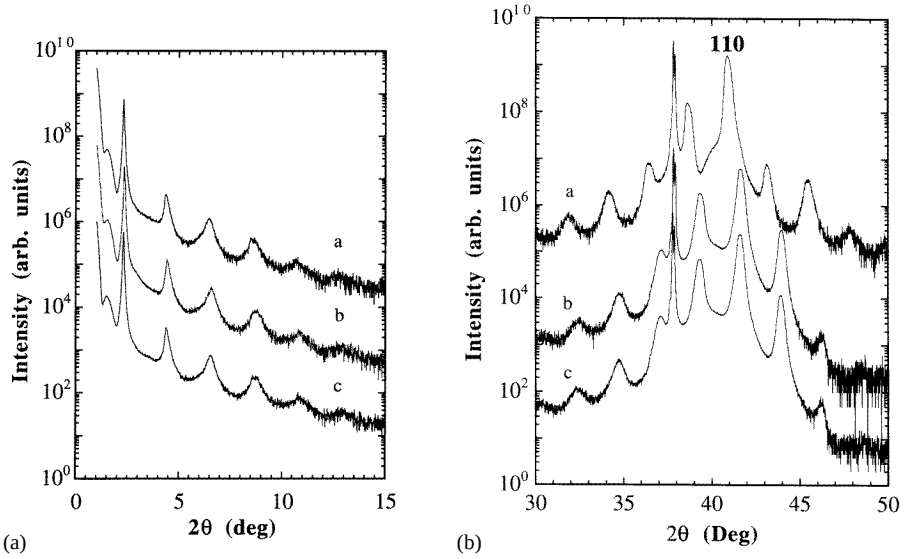

Figure 5. θ–2θ scans from (110) oriented samples. The hydrided sample with H/V = 0.5 is labelled **a** in the figures. The virgin sample is labelled **b**, and the dehydrided sample **c**. (a) The low-angle region. The diffractograms are shifted for clarity. The changes in the diffractogram are small; the change in Λ is only 1.5%. (b) The high-angle 110 Bragg peak region.

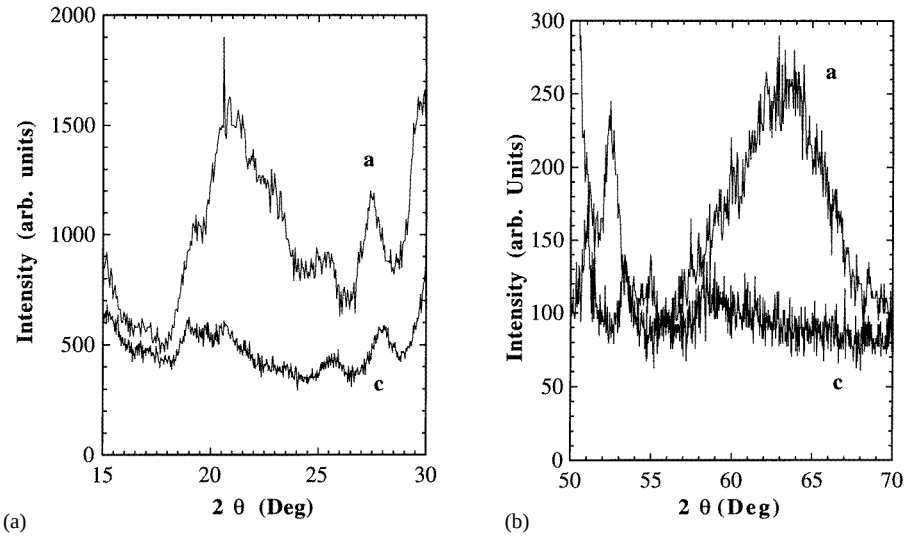

Figure 6. The expanded part of the diffractogram around (a) 20° and (b) 60° for the hydrided and the dehydrided sample. The peak in the hydrided sample indicates a superstructure in the sample with a periodicity of roughly twice the average lattice constant. The hydrided sample with H/V = 0.5 is labelled **a** in the figures, and the dehydrided sample **c**.

In figure 6 we display the 2θ region around 20 and 60° for the hydrided and the dehydrided (110) samples. A linear scale is chosen to emphasize the difference in the intensity between these scans. The intensity of the observed peaks is extremely weak compared to the main Bragg peak, indicating a weak modulation potential. The periodicity

of this modulation is roughly twice that of the average lattice parameter of the sample. The FWHM of the peak at 20.9° is approximately 2.5 and 5.8° for the peak at 63.5°, which corresponds to a coherence length of approximately 3 nm, using the Scherrer formula.

The results of XRD reciprocal space mapping from the multilayered superlattices were in qualitative agreement with the results presented above: a weak expansion in the growth direction with no change in the in-plane lattice parameter.

5. Discussion

The formation of ordered bulk vanadium metal hydride phases is relatively well understood [18–20]. At 300 K, there exist three phases, α, β and ε, in the concentration range $0 < \mathrm{H/V} \leqslant 1$ (atomic ratio) of interest here. The α phase is a disordered low-concentration cubic phase with tetrahedral occupation. In the tetragonal β-phase, hydrogen occupies sets of octahedral sites which form sheets perpendicular to the 110 direction. The change in the lattice parameters is anisotropic. The c-axis is expanded from 0.303 to 0.330 nm, and a and b are contracted to 0.300 nm. In the range $0.5 < \mathrm{H/V} < 0.8 (\beta + \varepsilon)$, the c-axis as well as the a- and b-axes expand linearly, by 3 and 1% respectively at 300 K [20]. For $\mathrm{H/V} = 0.5$, the population of the initially empty 110 sheets increases with temperature, and at 170 °C an ε-phase is formed. The characteristic sites for the ε-phase are therefore the same as for the β-phase, but no empty sheets are present. As the thicknesses of the hydrogen absorbing layers are extremely small, the comparison to the bulklike hydride formation must be made with some caution.

We divide the discussion into two parts. This is adequate, since at low concentrations the modulation of the effective potential can be treated by a simple argumentation based on the local interstitial electron density, while at high concentrations one has to consider the host mediated hydrogen–hydrogen interaction as well as the influence on the energy from the interaction with the substrate and the Mo clamping.

5.1. Low concentrations, $H/V \leqslant 0.1$

The main reasons for a different interstitial electron density in the V layers in Mo/V superlattices compared to that in bulk V are the observed increase of the x–y lattice parameters and charge transfer from Mo to V at the interfaces. The lattice parameter change can, in principle, be estimated from the measured average lattice parameters in the superlattice. For superlattices with Mo/V atomic ratio of 0.5, the volume of the unit cell is only 1% larger than the corresponding bulk value [16]. The lattice expansion leads to a decrease in the interstitial electron density and therefore increases the binding energy of H. This change will only modestly affect the shape of the effective potential in the samples. No direct information is presently available on the volume changes in coherent superlattices with Mo/V atomic ratio of 1.0, but by assuming a linear relation between the strain and the asymmetry, a tentative value of 1.5% is obtained. This implies at most a 1.5% decrease in the interstitial electron density, which corresponds roughly to 25 meV change in the effective potential, using the parametrized version of the effective medium theory [21].

In a theoretical work by Papadia *et al* [22], the interstitial electron density in coherent (001) Mo/V superlattices was calculated using the linear muffin-tin orbital method in the atomic-sphere approximation. The calculations were restricted to two modulation wavelengths, six and 10 monolayers. Later the calculations were extended to 12 monolayers [23]. The main result of relevance here is that the interstitial electron density was found to be altered in three monolayers on each side of the interfaces. Due to

higher interstitial electron density in V at the interfaces than in the interior region, it is not as energetically favourable for hydrogen to reside close to the interfaces. The interstitial electron density in the interior region of the V layers was found to be lower than the corresponding bulk value. A quantitative comparison of the effective potential for H in bulk V and a Mo/V superlattices is not possible, as the total energy was not minimized with respect to the out-of-plane lattice parameter, but a qualitative comparison is legitimate as the shift of the levels only modestly affects the extension of the interface region. The change of the heat of solution in the vicinity of the interfaces can be obtained within the effective medium theory [21], in which the energy of the embedded hydrogen atom is calculated using the obtained interstitial electron densities [22]. To our knowledge, no theoretical work has been reported on the interstitial electron densities in (110) oriented Mo/V superlattices.

The effective potential seen by the hydrogen in the interior of the V layers for the different modulation wavelengths is the same within a fraction of k_BT (differences $\ll 25$ meV) for both the (001) and (110) oriented multilayered superlattices, as seen from the way they are filled up at $T = 300$ K (see figure 3).

By applying Boltzmann statistics on a hypothetical two-level system, an energy difference of 25 ± 5 meV was obtained for the fourth and the third atomic planes from the interface in the (001) oriented samples [7]. The effective medium theory was used to estimate an electron density shift of 0.6×10^{-3} electrons au^{-3} (corresponding to 1.6%), using the value given for $\bar{n}_0$ in [22] for the interior vanadium layers. The population of the interfaces in the (110) oriented samples is somewhat different. At the lowest concentration, the population of the third atomic plane from the interface is found to be, within the precision of the measurement, the same as in the interior region. Thus, the energy difference between the third and the fourth atomic plane must be, following the argumentation above, much smaller than 25 meV. Therefore the interface region in the (110) samples consists of only two monolayers, i.e. roughly a distance of 0.43 nm compared to the three monolayers, i.e. 0.45 nm, or the (001) samples. It is therefore concluded that the charge transfer of the interstitial 'free electrons' scales as the distance, and not as the number of atomic planes.

5.2. Intermediate and high concentrations ($0.1 < H/V$)

The (001) and the (110) samples showed large differences in the concentration range 0.1–0.4. In the (110) oriented samples, no preferential population in the long-modulation subsamples was observed. This implies that the interaction energy must be repulsive or much smaller than k_BT (at room temperature). Recently, the enthalpy and the entropy for hydrogen in (001) Mo/V samples were measured. The host mediated hydrogen interaction was found to be attractive and close to that obtained for the β-phase in bulk samples [24] at $H/V < 0.5$. The enhanced interaction was attributed to the polarization of the elastic interaction of the hydrogen atoms. The polarization originates in the biaxial lattice strain and the clamping the vanadium layers. The implications of the elastic interaction and the boundaries on phase transitions are found in the work of Alfeld (see e.g. [25]).

To explore the origin of the orientation dependence, let us regard the possible local order of hydrogen in the V layers. A superstructure with a periodicity twice that of the average lattice constant is inferred in the (110) samples (see figure 6), and from the width of the peaks the coherence length of the superstructure is determined to be $\approx$3 nm, using the Scherrer equation. The extension of the superstructure is therefore roughly the same as the extension of a single V layer (3.4 nm). We can therefore consider the hydrogen atoms in one V layer as independent of the hydrogen in the rest of the superlattice. The Mo layers therefore act as clamping boundaries, and thereby prohibit elastic interaction

between the V layers. We first assume that the hydrogen planes are perpendicular to the 110 direction, as in the bulk β-$VH_{0.5}$, which is consistent with the XRD results. The nearest hydrogen neighbours belong therefore to the same (110) planes and the clamping implies that no coherent expansion can occur in the $1\underline{1}0$ or the $\underline{1}10$ directions, and no expansion can occur in the 001 direction due to the clamping effects. We can estimate the expected ratio of expansion for the two crystallographic orientations by requiring the same total internal elastic stress, and treating the monoclinic (110) samples as cubic. We also ignore the possible difference in the initial local free electron density of the two oriented samples. This is legitimate as the leading term in the expansion of the host is the elastic interactions of the hydrogen atoms [25]. The elastic energy density for a cubic crystal is [26]

$$w = \frac{1}{2}\sum_{ijkl} e_{ij} C_{ijkl} e_{kl} \tag{3}$$

where $e_{ij} = \frac{1}{2}[\partial u_i/\partial j + \partial u_j/\partial i]$. For the (001) oriented samples, all lattice response in the 100 and 010 orientations is zero due to the clamping and we obtain

$$w_{001} = \tfrac{1}{2} C_{11} e_{zz}^2. \tag{4}$$

The work which is required for a displacement for the (110) oriented sample can be obtained in an analogous manner:

$$w_{110} = \tfrac{1}{2}[C_{11}(e_{xx}^2 + e_{yy}^2) + 2C_{12}e_{xx}e_{yy} + 4C_{44}e_{xy}^2]. \tag{5}$$

The expansion is small and solely in the 110 direction, which implies $e_{xx} = e_{yy} \approx e_{xy}$. We measure the lattice response in the (110) direction, which for geometrical reasons is $\varepsilon_{110} = \sqrt{2}e_{xx}$. For the (001) samples $\varepsilon_{001} \equiv e_{zz}$. By requiring the elastic stress (σ) to be the same (using $\sigma = \delta w/\delta\varepsilon$), and assuming a linear relation between the hydrogen content and internal stress, we obtain

$$\varepsilon_{110}/\varepsilon_{001} \approx C_{11}/(C_{11} + C_{12} + 2C_{44}) \tag{6}$$

for a given hydrogen concentration in the samples. The resulting ratio is 0.52, using the values of the elastic constants from [27], compared to the obtained value of 0.65. Considering the gross simplifications in our approach, where we have for example assumed the same site occupancy of the hydrogen atoms (which gives the relation between the hydrogen content and the stress) and the initial strain of the lattices, the aggrement must be considered satisfactory.

At the lowest measured concentrations, the extension of the depleted region was found to be two monolayers. With increasing concentration, the extension of the depleted region seems to increase. To explore this feature, one has to distinguish between two situations.

Case 1. First, assume the coherence of the hydride phase regions to be limited by the steps present at the interfaces. These steps result in a thickness variation of the V layers, which is on average ± 1 monolayer [15]. Although the growth mode is layer by layer, the average thickness of the Mo and the V layers is not an integer number of atomic planes. This lack of phase locking results in steps, where the width of the terraces is governed by the diffusivity of the surface atoms. In the regions where such thickness variations are present, a disorder (mismatch) in the hydrogen planes must exist. These regions would therefore, by necessity, have lower hydrogen concentrations and are therefore expected to decrease the relative hydrogen content of the layers. However, as the step density is not expected to vary with the thickness of the V layers, such a disorder will not contribute to the observed increase in the depletion zone. Only a reduction of the interior concentration would emerge, which does not scale with the V thickness.

Case 2. If the in-plane correlation length of the hydride planes is larger than the step width of the V layers, additional 'dead regions' will be present. These dead regions are V islands at a three-monolayer distance from the Mo interface, which cannot be fully populated due to the lack of coherent expansion of these atomic planes. There are only islands of possible sites for the hydrogen atoms, which restricts the size of the phase regions in these planes. These islands will be equally populated as the interior regions at low concentrations, as the strain field is local for a disordered phase. At higher concentrations, it is more energetically favourable to expand coherently. This will result in a situation where the interior region can have higher concentrations than the islands in the vicinity of the interfaces. This additional dead layer will on average be one half of a monolayer at each interface, assuming random distribution of the steps.

Therefore, it is reasonable to conclude that the additional dead layer arises from the interplay between the interface steps at the ordering of the hydrogen in the (110) plane.

6. Summary

To summarize, the extension of the charge transfer region for the (110) samples is found to be two monolayers, which is roughly the same spatial distance as the three monolayers found in the (001) samples. With increasing concentration, the depletion zone is extended in the (110) samples. This increase is attributed to the influence of the thickness variation (± 1 monolayer) of the V layers on the ordered hydride phase.

The hydrogen induced volume change of Mo/V (110) superlattices is found to be smaller than that for the (001) oriented samples at room temperature. The ratio of expansion is found to be 0.65, compared to an estimated ratio of 0.52 from classical elastic theory. The elastic response and the clamping by the boundaries are the main causes for the reduced hydrogen induced expansion in the (110) samples.

The host mediated hydrogen–hydrogen interaction is inferred to be repulsive in the (110) samples, which should result in a disordered phase at room temperature. Hydrogen induced superstructure is observed perpendicular to the growth planes, with a coherence length (3 nm) which corresponds to the thickness of the hydrogen absorption layer (3.4 nm). These observations suggest a structure which is correlated in the 110 direction and disordered in the (110) plane.

Acknowledgment

Financial support from NFR and from the NUTEK/NFR materials research consortium on thin film growth is gratefully acknowledged.

Note added in proof. In a recent work (Andersson G, Hjörvarsson B and Isberg P 1997 *Phys. Rev.* B at press) the enthalpy and entropy changes of hydrogen in Fe–V superlattices was determined. The results proved the existence of a well defined energy state within the third monolayer of V from the interfaces. The energy difference was determined by absorption measurements of superlattices with different repeat lengths, the shortest consisting of only interface-like V layers. These results support the interpretation of the dead layer as originating from charge transfer, resulting in well defined interface states of hydrogen in metallic superlattices.

References

[1] Miceli P F, Zabel H and Cunningham J E 1985 *Phys. Rev. Lett.* **54** 917
[2] Miceli P F and Zabel H 1989 *Z. Phys.* B **74** 457

[3] Miceli P F and Zabel H 1987 *Phys. Rev. Lett.* **59** 1224
[4] Uher C, Cohn J L, Miceli P F and Zabel H 1987 *Phys. Rev.* B **36** 815
[5] Hjörvarsson B, Rydén J, Karlsson E, Birch J and Sundgren J-E 1991 *Phys. Rev.* B **43** 6640
[6] Hjörvarsson B, Vergnat M, Birch J, Sundgren J-E and Rodmacq B 1994 *Phys. Rev.* B **50** 11 223–6
[7] Hjörvarsson B, Ólafsson S, Stillesjö F, Karlsson E, Birch J and Sundgren J-E 1993 *Z. Phys. Chem.* **181** 343
[8] Ólafsson S, Hjörvarsson B, Stillesjö F, Karlsson E, Birch J and Sundgren J-E 1995 *Phys. Rev.* B **52** 10 792–5
[9] Karkut M G, Ariosa D, Triscone J-M and Fischer Ø 1985 *Phys. Rev.* B **32** 4800
[10] Ariosa D, Fischer O, Karkut M G and Triscone J M 1987 *Phys. Rev.* B **37** 3238
[11] Triscone J M, Ariosa D, Karkut M G and Fischer Ø 1988 *Phys. Rev.* B **35** 2421
[12] Birch J, Yamamoto Y, Hultman L, Radnoczi G, Sundgren J-E and Wallenberg L R 1990 *Vacuum* **41** 1231
[13] Birch J, Severin M, Wahlström U, Yamamoto Y, Radnoczi G, Riklund R, Sundgren J-E and Wallenberg L R 1990 *Phys. Rev.* B **41** 10 396
[14] Birch J, Hultman L, Sundgren J-E and Radnoczi G 1996 *Phys. Rev.* B **53** 8114–23
[15] Håkansson G, Birch J, Hultmann L, Ivaniv I P, Sundgren J-E and Wallenberg L R 1992 *J. Cryst. Growth* **121** 399
[16] Birch J, Sundgren J-E and Fewster P F 1995 *J. Appl. Phys.* **78** 11
[17] Stillesjö F, Hjörvarsson B and Zabel H *Phys. Rev.* B **54** 3079–83
[18] Velecckis E and Edwards R K 1969 *J. Phys. Chem.* **73** 683
[19] Scober T and Weizl H 1978 *Topics in Applied Physics (Hydrogen in Metals II)* vol 29 ed G Alefeld and J Völkl (Berlin: Springer) p 9
[20] Maeland A J 1964 *J. Phys. Chem.* **68** 2197
[21] Nörskov J K 1982 *Phys. Rev.* B **26** 2875
[22] Papadia S, Karlsson K, Nilsson P O and Jarlborg T 1992 *Phys. Rev.* B **45** 1857
[23] Papadia S 1994 private communication
[24] Stillesjö F, Ólafsson S, Isberg P and Hjörvarsson B 1995 *J. Phys.: Condens. Matter* **7** 8139–50
[25] Alfeld G 1972 *Ber. Bunsenges. Phys. Chem.* **76** 746
[26] See for example Feynman R P, Leighton R B and Sands M 1997 *The Feynman Lectures on Physics* vol II (Reading, MA: Addison-Wesley)
[27] Hellwege K H and Hellwege A M (eds) 1969 *Landolt–Börnstein New Series 1969* (Berlin: Springer) vol III/2